

The unusual near-infrared morphology of the radio-loud quasar 4C + 09.17

L. Armus,¹ G. Neugebauer,¹ M. D. Lehnert² and K. Matthews¹

¹Palomar Observatory, Caltech, Pasadena, CA 91125, USA

²Sterrewacht Leiden, Postbus 9513, 2300RA Leiden, The Netherlands

Accepted 1997 March 21. Received 1997 February 6; in original form 1996 October 7

ABSTRACT

Near-infrared images of the luminous, high-redshift ($z=2.1108$), radio-loud quasar 4C + 09.17 reveal a complex structure. The quasar ($K=15.76$ mag) is surrounded by three ‘companion’ objects having $17.9 < K < 20.2$ mag at radii of $1.7 < \Delta r < 2.9$ arcsec, as well as bright, diffuse emission. The brightest companion has a redshift of $z=0.8384$ (Lehnert & Becker), and its optical–infrared colours (Lehnert et al.) are consistent with a late-type spiral galaxy at this redshift with a luminosity of about $2L^*$. This object is probably the galaxy responsible for the strongest Mg II absorption-line system seen in the spectrum of 4C + 09.17 by Barthel et al. Redshifts are not available for the remaining two companions. The red colours of the second brightest companion appear most consistent with a high-redshift star-forming galaxy at $z > 1.5$. If this object is at the redshift of 4C + 09.17, it has a luminosity of about $7L^*$. The faintest companion has colours which are unlike those expected from either a spiral or an E/S0 galaxy at any redshift associated with the 4C + 09.17 system. Since this object lies along the same direction as the radio jet/lobe of 4C + 09.17, as well as the extended Ly α emission mapped by Heckman et al., we suggest that this component can be explained as a combination of strong line emission and scattered QSO light. The resolved, diffuse emission surrounding 4C + 09.17 is bright, $K \sim 17.0$ mag, and about 1 mag redder in $J - K$ than the quasar. If this emission is starlight, a very luminous elliptical host galaxy is implied for 4C + 09.17. Scattered and reddened AGN light, emission-line gas, and flux from absorbing galaxies along the line of sight may all contribute to this emission.

Key words: galaxies: photometry – quasars: general – quasars: individual: 4C + 09.17 – infrared: galaxies.

1 INTRODUCTION

At low redshifts, quasars often sit at the centres of luminous galaxies (Hutchings, Crampton & Campbell 1984; Smith et al. 1986; Bahcall et al. 1997). In general, radio-loud quasars (i.e., those with monochromatic radio powers at centimetre wavelengths of more than 10^{25} – 10^{26} W Hz^{−1} and radio-to-optical monochromatic luminosity ratios larger than ~ 100 ; see Kellerman et al. 1988 and Schneider et al. 1992) inhabit elliptical galaxies, while radio-quiet quasars tend to be found in spiral galaxies (Boroson & Oke 1984; Malkan 1984; Boroson, Persson & Oke 1985; Smith et al. 1986). Furthermore, the host galaxies of radio-loud quasars tend to be more luminous by about 1 mag in the visual than their

radio-quiet counterparts (Smith et al. 1986). The reasons for these apparent dichotomies are not well understood. Images of low-redshift, luminous ($M_b < -23$ mag) quasars obtained with the *Hubble Space Telescope* (HST) show a wide variety of host galaxy morphologies, including both elliptical and spiral systems as well as highly disturbed galaxies which may be interacting with and/or accreting close companions (Disney et al. 1995; Hutchings & Morris 1995; Bahcall et al. 1997). In addition, recent deep infrared imaging (McLeod & Rieke 1995; Neugebauer, Matthews & Armus 1995) has proven very effective in finding smooth host galaxies and faint companions around some low-redshift quasars. That the nature of quasar host galaxies even at low redshift is still a matter of some debate is evidenced by

the recent discussions concerning the *HST* results presented by Bahcall et al., and the efforts made to reconcile these results with ground-based measurements made at longer wavelengths (e.g. McLeod & Rieke 1995). In particular, the fact that 50 per cent of the radio-quiet quasars imaged by Bahcall et al. seem to have elliptical hosts has challenged the apparent clear-cut distinction between the hosts of radio-quiet and radio-loud quasars.

At redshifts above $z \sim 2$, disentangling host galaxy light from AGN light is made difficult by the relative faintness of the host galaxy as well as the blurring effects of atmospheric seeing. However, it is precisely at these redshifts that studies of the near environments of quasars offer the most hope of furnishing clues to the early evolution of AGN and galaxies. It is now well established that the redshift regime of $z \sim 2-3$ represents a real maximum in the number density of luminous quasars (Hartwick & Schade 1990; Schmidt, Schneider & Gunn 1995). Between these redshifts and the present, the number density of luminous quasars has dropped by more than a factor of 1000, suggesting very strong cosmic evolution. If high-redshift quasars sit at the centres of luminous host galaxies, the peak in the quasar density at $z \sim 2-3$ may signal an epoch where luminous galaxies were being hierarchically assembled (e.g. Carlberg & Couchman 1989).

As part of a *K*-band imaging survey of the Mpc-scale environments of a large sample of high-redshift quasars with the W. M. Keck Telescope, we have imaged a very complex system around the $z=2.1108$, radio-loud quasar 4C + 09.17 at RA(1950) = $04^{\text{h}}45^{\text{m}}37^{\text{s}}.12$, Dec.(1950) = $+09^{\circ}45'37''.2$. This object serves as an excellent example not only of the wealth of detail that a deep imaging programme of this magnitude will provide, but also of the various pitfalls associated with inferring the properties of the host galaxies and companions of high-redshift quasars.

4C + 09.17 was previously found to have an extended, asymmetric Ly α nebula with a luminosity of about 1.6×10^{44} erg s $^{-1}$ by Heckman et al. (1991). Lehnert et al. (1992) imaged 4C + 09.17 in the *K* band and found resolved emission at radii from 1 to 6 arcsec with a $K \sim 17.5 \pm 0.4$ mag. This emission appeared asymmetric, but the true morphology of the nebula was unclear. The Keck *J*- and *K*-band data presented here show a group of three objects within 3 arcsec of the quasar as well as very bright diffuse near-infrared emission, and they allow a determination of the magnitudes and colours for each of the components.

Barthel, Tytler & Thomson (1990) quote a number of emission-line redshifts for 4C + 09.17 from the C iv, He II and C III features, spanning a range of $z = 2.1085$ to 2.1114 . We adopt the average emission-line redshift of $z = 2.1108$, as determined by Barthel et al., as the systemic redshift of 4C + 09.17. In addition to the emission lines, there are four absorption-line systems in the spectrum of 4C + 09.17 (Barthel et al. 1990). Two of these are Mg II systems at redshifts of $z = 0.839$ and 1.466 , the former being significantly stronger than the latter, with rest-frame equivalent widths (EWs) of 2.68 and 0.46 Å, respectively. In addition, there is a C iv absorption system at a redshift of $z = 2.107$, having a rest-frame EW of 2.3 Å. Finally, there is a C iv absorption-line system with $z_{\text{abs}} \sim z_{\text{em}}$ and a rest-frame EW of 1.4 Å.

Throughout this paper we adopt $H_0 = 75$ km s $^{-1}$ Mpc $^{-1}$ and $q_0 = 0$, so that the distance to 4C + 09.17 is 5576 Mpc, and 1 arcsec on the sky is equivalent to 8.8 kpc in projection.

In order to compare the observed infrared magnitudes to the expected rest-frame values of typical galaxies in the local Universe, we employ the optical luminosity function of Mobasher, Sharples & Ellis (1993), such that a spiral galaxy has a characteristic absolute magnitude, $M_B^* = -20.49$ mag, while an E/S0 galaxy has a characteristic absolute magnitude, $M_B^* = -20.24$ mag, following Schechter (1976), and converting the Mobasher et al. values into ones appropriate for an $H_0 = 75$ km s $^{-1}$ Mpc $^{-1}$. Combining these characteristic absolute magnitudes with the spectral energy distributions of Coleman, Wu & Weedman (1980), we estimate that the apparent *K* magnitudes of an L^* spiral and E/S0 galaxy at a redshift of $z = 2.1108$ are $K = 21.46$ and 20.99 mag, respectively.

2 OBSERVATIONS AND DATA REDUCTION

Observations of 4C + 09.17 were made at the W. M. Keck Observatory on the nights of 1995 February 13 and October 5 UT with the Near-Infrared Camera (NIRC). The quasar was imaged through a broad-band *K* filter ($2.0-2.45$ μm) during both runs, and through a broad-band *J* filter ($1.12-1.37$ μm) during the 1995 October observing run. The plate scale of the 256×256 InSb array is 0.15 arcsec per pixel. The total integration time through the *K* filter was 1080 s in 1995 February and 540 s in 1995 October. The total integration time through the *J* filter was 540 s in 1995 October. In each case, individual images of 60-s duration have been taken with the quasar moved by ~ 10 arcsec on the array between successive exposures. Sky and flat-field frames were generated from the data by combining exposures in groups of 7–9 using either a clipped mean or median filtering technique. An offset guider employing a visual wavelength CCD was used to accurately maintain the telescope tracking. Since the quasar is visible in each 60-s exposure, centroids were measured for the individual frames and used to derive the offsets used to create the final *K*- and *J*-band mosaics. In addition to the quasar, observations were made of a nearby ($\Delta r = 11$ and 5 arcmin) star either immediately before (1995 October data) or immediately after (1995 February data) the observations of the quasar, respectively, in order to obtain an estimate of the point-spread function (PSF). During both observing runs the PSF star was imaged in a manner identical to that used for the quasar itself, using the same raster pattern and exposure times (60 s per position). From these PSF images the seeing was estimated to be approximately 0.7 and 0.5 arcsec full-width at half-maximum (FWHM) during the 1995 February and October observations of 4C + 09.17, respectively. The conditions were photometric during both observing runs, and observations of UKIRT faint standard stars (Casali & Hawarden 1992) provided the flux calibration. Although the seeing was steady during the 1995 October observing run, it degraded noticeably to 0.9–1.0 arcsec FWHM during the observations of the standard stars on the 1995 February run, making small-aperture fluxes derived from the latter data set uncertain. Although both data sets are combined to obtain the deepest possible images of 4C + 09.17 (Fig. 1), only the 1995 October data set is used to derive magnitudes for the individual components and to assess the nature of the extended emission in the 4C + 09.17 system (Figs 2 and 3).

4C +09.17

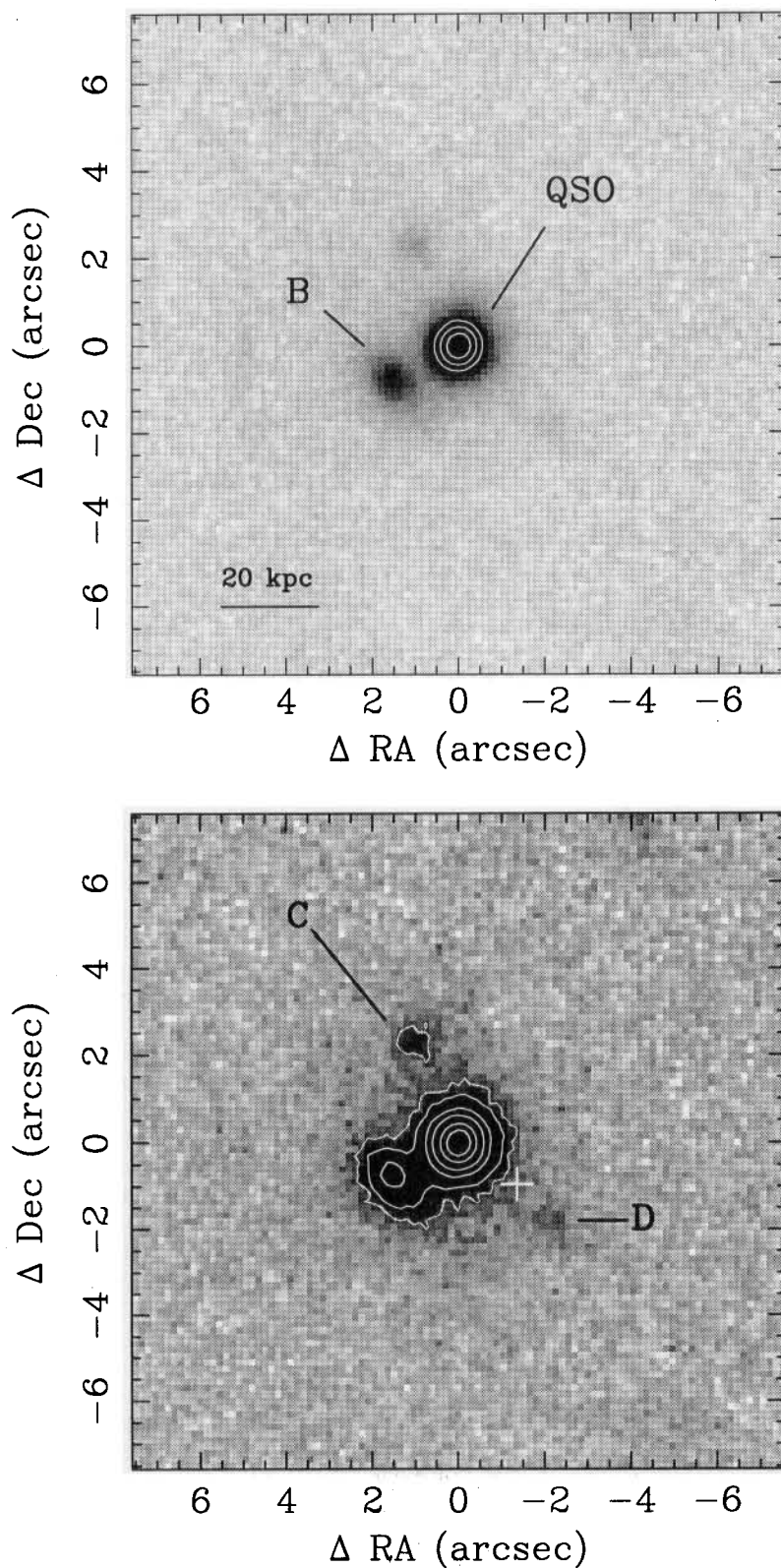


Figure 1. Two views of 4C +09.17 in the K band. In the top panel, the colour palette has been chosen to highlight the quasar (component 'A') and the brightest of the near-infrared companions (component 'B'). A solid bar depicting a projected scale of 20 kpc at the redshift of the quasar (for $H_0 = 75 \text{ km s}^{-1} \text{ Mpc}^{-1}$ and $q_0 = 0$) is also shown. In the bottom panel, the colour palette has been chosen to highlight the diffuse emission surrounding the system, as well as components 'C' (at 1, 2) and 'D' (at -2, -2). A cross marks the position of the radio lobe mapped by Barthel et al. (1988) and Lonsdale, Barthel & Miley (1993), assuming that the brightest radio component is coincident with the quasar. Component 'D' lies along the same direction from the quasar as the radio jet, yet at a larger distance than the radio lobe. In both images, north is up and east is to the left.

Visual images of the 4C + 09.17 system were obtained with the *HST* using the Wide Field and Planetary Camera (WFPC2) on 1994 September 9. These images were taken through the F555W filter. The observations of 4C + 09.17, along with the results from observations of five other high-redshift QSOs with *HST*, are fully described in Lehnert et al. (1997, in preparation). The 4C + 09.17 data are included here in order to derive the visual–infrared colours of the system.

The Galactic colour excess towards 4C + 09.17 is $E(B - V) \sim 0.16$ mag (Burstein & Heiles 1982). Using the reddening curves of Savage & Mathis (1979) and Rieke & Lebofsky (1985), we derive a Galactic extinction of $A_V = 0.5$ mag, $A_J = 0.14$ mag and $A_K = 0.06$ mag, respectively. The data presented in the following sections are corrected for these extinctions.

3 RESULTS

The infrared observations reveal a complex structure surrounding the $z = 2.1108$, radio-loud quasar 4C + 09.17. The quasar resides in a system containing three distinct components visible at $2.2 \mu\text{m}$, in addition to a resolved, diffuse nebula. The composite *K*-band mosaic made from the combined 1995 February and October data sets is shown in Fig. 1. The brightest companion, 1.72 arcsec south-east of the quasar and hereafter labelled as component ‘B’, is clearly resolved, with a structure that appears elongated in the north-east–south-west direction. This object has a *K* magnitude of 17.87 ± 0.03 , and a colour of $J - K = 1.56 \pm 0.04$ mag as measured through a 2.0-arcsec diameter circular beam centred on the emission peak. For comparison, the quasar itself (component ‘A’) has a *K* magnitude of 15.76 ± 0.03 and a colour of $J - K = 1.46 \pm 0.04$ mag. Component ‘C’, located 2.54 arcsec north-east of the quasar, has a *K* magnitude of 19.42 ± 0.07 , and a colour of $J - K = 2.16 \pm 0.15$ mag. Component C is the reddest member of the 4C + 09.17 system. Finally, there is a very faint, diffuse emission region approximately 3 arcsec south-west of the quasar. This emission has a local maximum, labelled ‘D’ in Fig. 1, approximately 2.9 arcsec from the quasar, with a *K* magnitude 20.15 ± 0.13 and a $J - K$ colour of 1.17 ± 0.17 mag. Component D is found along the direction of the radio jet mapped

at 15 GHz by Barthel et al. (1988) and Lonsdale, Barthel & Miley (1993), but is at a larger distance from the quasar than the radio lobe at a radius of 1.6 arcsec – marked with a cross in the lower panel of Fig. 1. The magnitudes and colours of the quasar and its companions, corrected for Galactic extinction, are listed in Table 1.

It is clear from Fig. 1 that the entire 4C + 09.17 system is surrounded by diffuse infrared emission. In Fig. 2(a), we plot the azimuthally averaged *K*-band surface brightness of the 1995 October data out to a radius of 4.5 arcsec. For comparison, the same quantity as a function of radius is plotted for the PSF star taken immediately before the quasar observations. Both profiles have been normalized to the flux within the central three pixels, or 0.45 arcsec. Excess emission above that expected from a point source is clearly seen at all radii. The ‘bump’ in the quasar surface brightness distribution at about 1.5 arcsec is caused by component B. For comparison, the *K*-band surface brightnesses of the quasar and PSF star calculated over a restricted sky position angle of $262^\circ < \text{PA} < 352^\circ$ (measured east from north) to exclude components B, C and D from the average are plotted in Fig. 2(b). The excess over the PSF image is still obvious when the contributions from the quasar companions are removed.

From estimates of the amount of resolved emission in the *J*- and *K*-band images, constraints can be placed on the luminosity and colour of the emission around 4C + 09.17. The FWHM of the PSF images were about 0.5 arcsec in both the *J* and *K* filters during the 1995 observations. An estimate of the fraction of the total emission which is resolved around 4C + 09.17 has been made by scaling the flux found within a radius of 0.37 arcsec (2.5 pixel) in the QSO image to that found in the PSF image. Since there is asymmetric structure around 4C + 09.17 due to components B, C and D, we have performed this calculation over the same restricted angle used to generate Fig. 2(b). In the *K* band, approximately 27 per cent of the total emission beyond a radius of 0.37 arcsec is resolved, while in the *J* band the fraction is about 11 per cent. The total magnitudes of the 4C + 09.17 system measured in 8 arcsec diameter circular beams centred on the QSO (corrected for Galactic extinction) are $K = 15.45$ mag and $J = 16.94$ mag. After removing the contributions of components B, C and D to the total flux, the resolved emission around 4C + 09.17 (beyond a radius of 0.37 arcsec) has $K \sim 17.0$ mag and $J \sim 19.5$ mag. This is slightly brighter than the measurement of Lehnert et al. (1992).

In Fig. 3, the infrared and visual flux densities, normalized to the flux density at an observed wavelength of $2.2 \mu\text{m}$, are shown for components B, C and D, as well as the quasar itself. These are overlaid on four representative spectral energy distributions (observed Im, Scd, Sbc and E/S0 galaxy spectra) taken from Coleman et al. (1980), which have been redshifted to $z = 2.1108$ (Fig. 3a) and $z = 0.84$ (Fig. 3b). The rest-frame UV data have been corrected for Galactic extinction by Coleman et al.

4 DISCUSSION

The apparent quasar companions are most likely to originate in one of the following ways. First, each could be a foreground galaxy, possibly associated with one or more of

Table 1. Near-infrared magnitudes and colours of the components in the 4C + 09.17 system. All values are measured through circular beams of 2.0-arcsec diameter. Column 1 is the designation used in the text. Column 2, Δr , is the distance of the component from the quasar.

Components in the 4C + 09.17 System				
Component	Δr	<i>K</i>	<i>J</i> – <i>K</i>	<i>V</i> – <i>K</i>
"	"	mag	mag	mag
A=QSO	0.0	15.76 ± 0.03	1.46 ± 0.04	3.57 ± 0.04
B	1.7	17.87 ± 0.03	1.56 ± 0.04	4.69 ± 0.07
C	2.1	19.42 ± 0.07	2.16 ± 0.15	> 5.35
D	2.9	20.15 ± 0.13	1.17 ± 0.17	4.40 ± 0.24

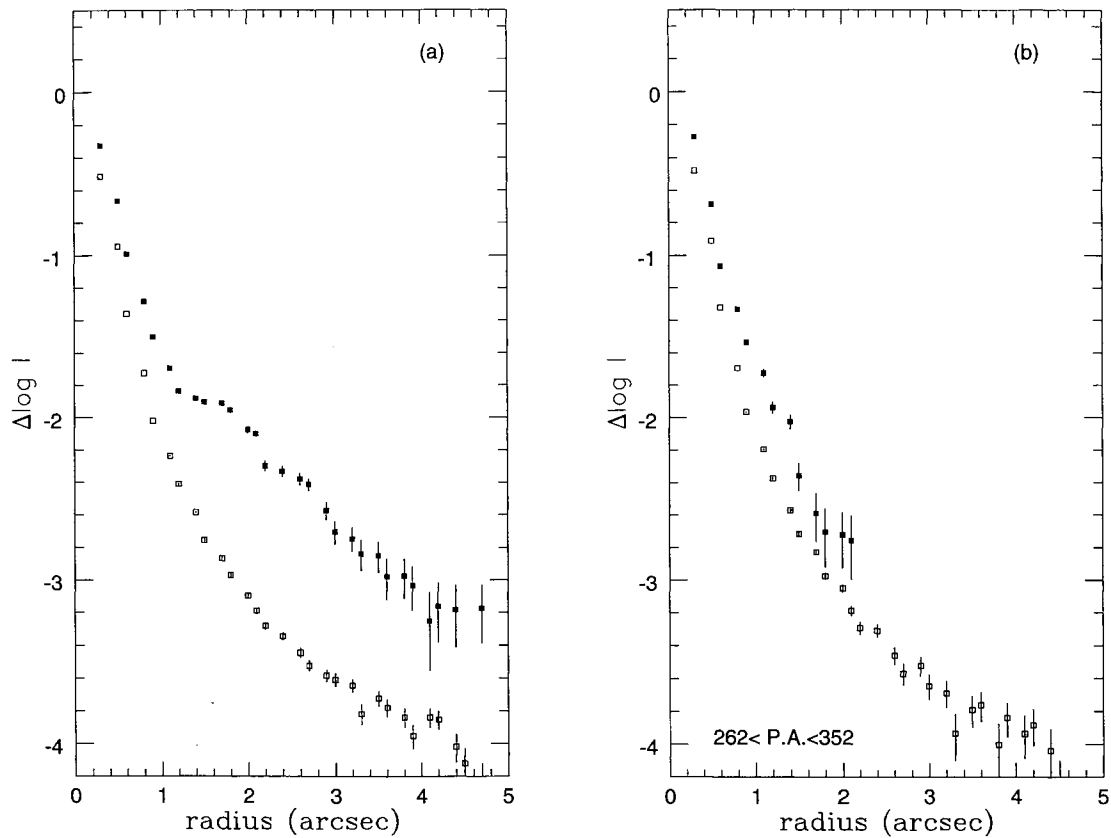


Figure 2. Azimuthally averaged K -band surface brightness profile of 4C + 09.17 in units of relative flux per pixel. In (a) the light is averaged over all angles. In (b) the average is restricted to $262^\circ < \text{PA} < 352^\circ$, chosen to exclude the contribution from components B, C and D from the average. In both cases the quasar is shown as solid squares and the point-spread function (PSF) is shown as open squares. The quasar and the PSF have been normalized to contain the same number of counts within the central 0.45 arcsec.

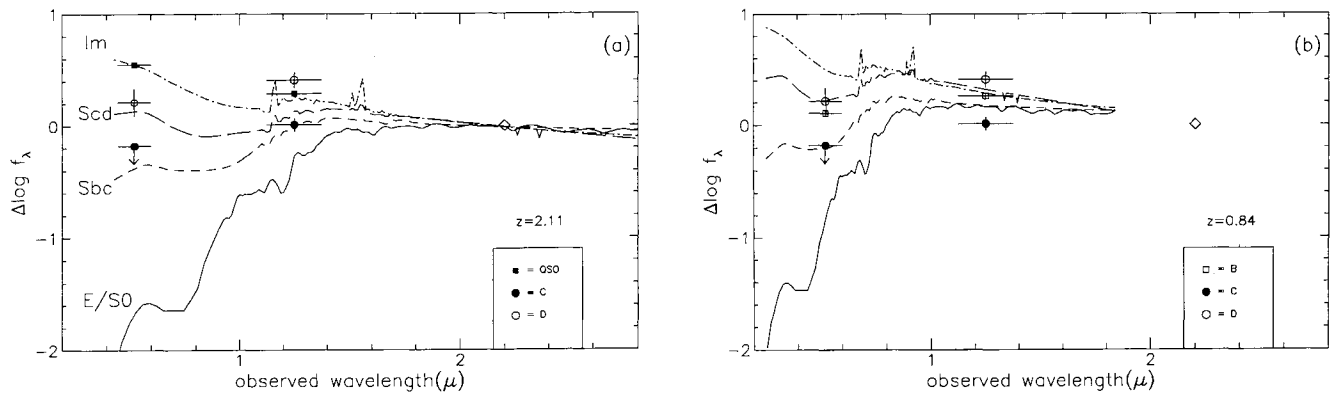


Figure 3. The optical–near infrared flux densities (normalized to the K -band flux density) of the components in the 4C + 09.17 system, corrected for a Galactic extinction of $A_V = 0.5$ mag, and overplotted on representative galaxy spectral energy distributions taken from Coleman, Wu & Weedman (1980). The Im galaxy spectrum is a composite of NGC 4449 and 1140, the Scd galaxy spectrum is a composite of M33 and NGC 2403, the Sbc galaxy spectrum is a composite of M51 and NGC 2903, and the E/S0 galaxy spectrum is a composite of the bulges of M31 and M81. All UV spectral points have been corrected for Galactic extinction. The energy distributions have been extended into the near infrared for Fig. 3(b) by matching the $J-H$ and $H-K$ colours of spiral and elliptical galaxies from Aaronson (1977) to the $I-J$ colours of models with the closest SED match in Bruzual & Charlot (1993). Two redshifts are depicted here, $z = 2.1108$ (a) and $z = 0.839$ (b), corresponding to the redshift of the quasar as well as the strongest Mg II absorption-line system seen in the spectrum of 4C + 09.17 by Barthel et al. (1990), respectively. The observed F555W point for component C is an upper limit. The diamond symbol in each plot marks the centre of the observed K -band window, to which the individual spectra have been normalized.

the absorption-line systems seen in the spectrum of 4C+09.17 by Barthel et al. (1990). The three $z_{\text{abs}} \ll z_{\text{em}}$ (Mg II and C IV) absorption-line systems in the quasar spectrum provide potential redshifts for the nearby companions. Secondly, any or all of the companions could be at the same redshift as the quasar, possibly interacting with or accreting on to the quasar host galaxy. If they are at the redshift of 4C+09.17, starlight, ionized gas and/or scattered AGN light could contribute to the measured infrared fluxes. We deal with each of the infrared components separately below in the light of these possibilities.

4.1 Component B

Component B has recently been shown to be a redshift of $z=0.8384$ from an identification of the [O II] 3727-Å emission line by Lehnert & Becker (1997, in preparation). This redshift is consistent with the idea that component B is responsible for the strongest Mg II absorption-line system in the spectrum of 4C+09.17. At this redshift, the separation on the sky of component B and 4C+09.17 (the Mg II ‘impact parameter’) is about 11.6 kpc. The empirical relationship between impact parameter and rest-frame Mg II EW found by Lanzetta & Bowen (1990) predicts a separation of 8–10 kpc between 4C+09.17 and the absorbing galaxy producing the Mg II absorption line, when their data are converted to an $H_0=75 \text{ km s}^{-1} \text{ Mpc}^{-1}$. The optical–infrared colours of component B are most similar to those of a late-type spiral galaxy at $z \sim 0.8$ (Fig. 3b). In Fig. 4, the $V-J$ versus $J-K$ colours of the galaxy templates used in Fig. 3 are plotted as a function of redshift from $z=0$ to 2.2 in steps of $\Delta z=0.2$. Also shown in Fig. 4 are three reddening vectors corresponding to the change in $J-K$ and $V-J$ for a rest-frame $A_V=1.0$ mag at $z=0$, 1.0 and 2.0. The galaxies

used as templates for the Im, Scd, Sbc and E/S0 Hubble types by Coleman et al. (1980) are shown as observed, i.e., they include intrinsic reddening. Component B can be reconciled with the Scd curve with a slight amount ($A_V \sim 0.5$ mag) of extra reddening. The J -band magnitude of component B ($J \sim 19.4$) corresponds to a monochromatic luminosity of about $2L^*$ at a rest-frame wavelength of 6800 Å. The infrared and visual fluxes are therefore consistent with component B being a late-type spiral galaxy at $z=0.84$.

4.2 Component C

Due to its proximity (at least in projection), it is natural to ask whether component C could be associated with component B. Component C could be a galaxy at $z \sim 0.8$, yet it is redder than even an old stellar population at this redshift (see Figs 3b and 4). The $J-K$ and $V-J$ colours of component C imply that the source lies at a fairly large redshift, i.e. $z \geq 1.5$. Although the (3σ) limit on the V magnitude prohibits an accurate estimate of the $V-J$ colour of component C, it appears that the colours can be matched by either the Im or the spiral galaxy templates by varying the amount of reddening, as long as the galaxy is at a high redshift. If component C is at the redshift of 4C+09.17, it may be a $7L^*$ spiral at a projected separation of about 18 kpc. The colours of component C are consistent however, given the $V-J$ limit and the uncertain reddening, with a spiral galaxy at the redshift of the $z=1.4664$ Mg II absorption-line system in the spectrum of 4C+09.17. Using the relationship between impact parameter and Mg II absorption equivalent width (Lanzetta & Brown 1990), the EW of 0.46 Å would predict a separation of about 40 kpc between component C and the quasar. The measured separation is 2.1 arcsec, or only 17 kpc at $z=1.466$, implying an expected rest-frame

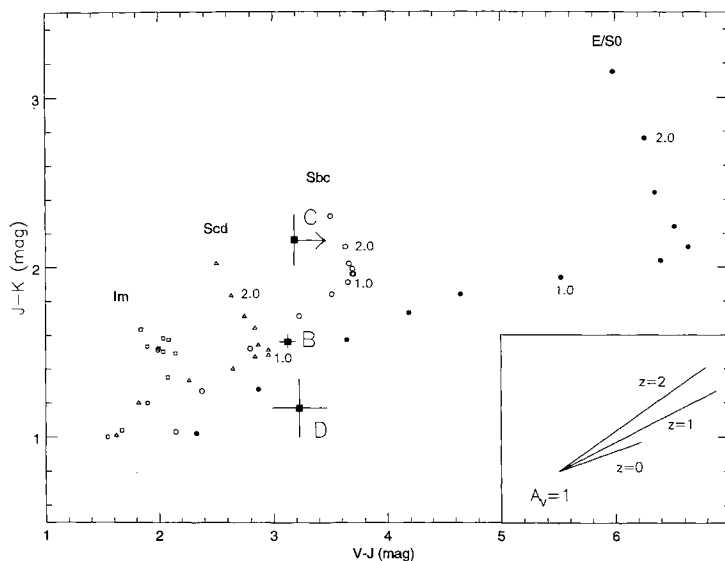


Figure 4. The $V-J$ versus $J-K$ colours of components B, C and D overplotted on the colours expected from the basic galaxy types of Fig. 3 (from Coleman, Wu & Weedman 1980) as a function of redshift between $0 < z < 2.2$, in steps of $\Delta z=0.2$. The Im galaxy is given by open squares, the Scd galaxy by open triangles, the Sbc galaxy by open circles, and the E/S0 galaxy by solid circles. The data for components B, C and D are indicated by solid squares and labelled accordingly. The Scd, Sbc and E/S0 points corresponding to $z=1$ and 2 are labelled. In addition, three reddening vectors are shown corresponding to additional extinctions of $A_V=1$ mag in the rest-frame of an object at $z=0$, 1 and 2. The red colours of C indicate a high-redshift galaxy, while the colours of D are difficult to fit with any of the generic galaxy types. The optical–infrared colours of component B are consistent with a late-type spiral galaxy at $z \sim 0.84$.

EW of 1.0–1.5 Å. If component C is a spiral galaxy at $z = 1.466$, it has a relatively weak Mg II absorption-line system (for its measured impact parameter) and a luminosity of about $2L^*$.

4.3 Component D

Component D is fainter and bluer than components B and C. The combination of blue $J - K$ and red $V - K$ colours are quite unlike those expected for a galaxy at the redshift of component B (see Figs 3b and 4). It is clear from Fig. 4 that simply reddening any of the galaxy templates will not reproduce the colours of D. Within the uncertainties, the $V - J$ colours of D and B are the same, but D is about 0.3–0.4 mag bluer in $J - K$. If component D is at the redshift of component B, the H α line is redshifted to 1.208 μm , and lies in the J -band atmospheric window. This line (or more specifically, the H α + [N II] blend) could therefore contribute to the blue $J - K$ colour of component D, since there is no correspondingly strong line which is redshifted into the K -band window. To increase the brightness of component D by 0.3 mag would require an H α + [N II] line flux of about 5.3×10^{-16} erg cm $^{-2}$ s $^{-1}$, corresponding to a luminosity of about 1.4×10^{42} erg s $^{-1}$ at $z = 0.84$. This hypothesized line would have an intrinsic equivalent width of about 420 Å, large even for luminous, high-redshift radio galaxies (e.g. Eales & Rawlings 1993). Furthermore, if component D were a spiral galaxy at $z = 0.84$, it would be intrinsically very faint at about $0.3L^*$. The large H α + [N II] luminosity required to account for the blue $J - K$ colours of D coupled with its intrinsically faint overall luminosity make it unlikely that D is a galaxy at $z = 0.84$.

Since D is located along the radio jet/lobe axis of 4C + 09.17, and there is known extended Ly α emission-line gas at the location of component D which is probably ionized by the quasar, it is unlikely that D is at $z = 0.84$. It is most plausible to suggest that component D is at the redshift of 4C + 09.17. If D is at $z = 2.1108$, H α can contribute to the K -band flux at 2.04 μm , and [O II] 3627 Å can contribute to the J -band flux at 1.16 μm . Heckman et al. (1991) find extended UV continuum and Ly α emission surrounding 4C + 09.17. The resolved Ly α flux is $\sim 4 \times 10^{-15}$ erg cm $^{-2}$ s $^{-1}$, corrected for a Galactic extinction of 0.7 mag at 3800 Å (Burstein & Heiles 1982; Savage & Mathis 1979). If the ionized gas around 4C + 09.17 has the same Ly α -to-H α emission-line flux ratio as found in high-redshift radio galaxies, i.e., 3.5 (McCarthy, Elston & Eisenhardt 1992), the expected resolved H α flux is approximately 10^{-15} erg cm $^{-2}$ s $^{-1}$. Heckman et al. note that the resolved Ly α emission in 4C + 09.17 is not distributed symmetrically, but is extended more towards the south-west – the direction of both the radio jet and component D. Inspection of their fig. 1 shows that the radio lobe and component D lie well within the brightest extended Ly α emission line nebula. It is likely therefore, that any emission-line contribution to component D comes from gas ionized by the quasar.

As an upper limit to the contribution of emission lines to the K -band flux of component D, we can assign to it all the resolved H α emission-line flux estimated from the measured, resolved Ly α emission. When this is done, nearly 73 per cent of the flux from component D could be from H α , and the corrected continuum light has a $K \sim 20.8$ mag. Per-

forming the same calculation for [O II], and assuming that the Ly α -to-[O II] emission-line flux ratio is the same in 4C + 09.17 as it is in radio galaxies, namely about 8.5 (McCarthy 1993), we estimate that at most 22 per cent of the J -band light seen from component D could be [O II] emission – not as large a fraction as estimated for H α , but still significant.

Subtracting the maximum emission-line contributions from the measured J - and K -band fluxes makes the continuum $J - K$ colour of component D bluer than the redshift Im galaxy spectral energy distribution in Fig. 3(a). If the maximum emission-line contribution is used, the continuum from component D is too blue to be starlight at the redshift of 4C + 09.17. This conclusion is strengthened if resonant scattering of Ly α photons is an important effect, since then the H α line flux would be larger than we have estimated by using the measured Ly α line flux from Heckman et al. (1991). On the other hand, the H α emission-line contribution to the K -band flux of component D may be an upper limit for two reasons. First, the Ly α nebula mapped by Heckman et al. appears larger and more diffuse than component D, so the line emission is probably not concentrated in one area. Secondly, the H α emission line is near the edge of the K -band atmospheric window at 2.04 μm , and thus the contribution of this line to the integrated K magnitude is dependent upon the kinematics of the emission-line gas. None the less, it appears that if component D is at the redshift of 4C + 09.17 and emission lines are contributing to the broad-band, near-infrared fluxes, the blue continuum colours are inconsistent with starlight. If component D is the redshift of 4C + 09.17, its continuum flux may be dominated by reflected AGN light and emission lines energized by the quasar.

4.4 The diffuse emission around 4C + 09.17

In most cases, symmetric, diffuse emission around high-redshift quasars is assumed to be at the redshift of the quasar, since the likelihood of finding a foreground faint galaxy perfectly centred on the background quasar is very small. The symmetric emission can be starlight, emission-line gas, or scattered AGN light. The complex morphology of 4C + 09.17 and the coincidence of strong, redshifted emission lines forces us to consider all of these possibilities.

The resolved, diffuse emission beyond a radius of 0.37 arcsec (Fig. 2b) has a magnitude $K \sim 17.0$ mag and a colour $J - K \sim 2.5$ mag. This is redder in $J - K$ than any other component in the 4C + 09.17 system. The red $J - K$ colour of the extended emission seems inconsistent with a strong contribution from scattered AGN light at these wavelengths, unless the scattered light is heavily reddened by dust along the line of sight. If the diffuse emission is starlight, it is extremely luminous, and most similar in colour to an evolved stellar population. A K -band magnitude of $K \sim 17.0$ mag implies a $39L^*$ E/S0 host galaxy for 4C + 09.17. This luminosity is, in fact, a lower limit on the true luminosity of the 4C + 09.17 host galaxy, since the measurement is made beyond a radius of 0.37 arcsec from the quasar. At $z = 2.1108$, 0.37 arcsec corresponds to about 3.2 kpc. If the host galaxy follows an $r^{1/4}$ light profile (de Vaucouleurs 1948) with an effective radius of about 4 kpc (Kormendy

1977), the total luminosity of the 4C+09.17 host galaxy could be as much as $70\text{--}80L^*$. Although extended emission around other high-redshift quasars has been taken as evidence for extremely luminous ($>20L^*$) host galaxies by Lehnert et al. (1992), in the case of 4C+09.17 there are known absorption-line systems along the line of sight, implying that some of the light around the quasar must be in the foreground. Component B, which we have associated with the Mg II absorption system at $z=0.84$ is clearly extended. If this galaxy is symmetric, at least in the direction toward and away from 4C+09.17, we estimate that about 10 per cent of its total emission lies at a radius of greater than 2.0 arcsec, i.e., at a large enough distance to contribute to the diffuse emission around the quasar. This flux from component B could be responsible for about 6 per cent of the resolved emission around 4C+09.17. If component B is highly asymmetric toward 4C+09.17, perhaps as a result of a galactic arm or tidal tail, the contribution could be larger than 6 per cent, although it seems not to be a dominant effect.

There is certainly resolved emission-line gas around 4C+09.17, as evidenced by the spatially resolved Ly α imaging presented by Heckman et al. (1991). In principle, H α , [N II] and [S II] emission may contribute to the integrated K -band light seen surrounding the quasar. However, even if all the resolved Ly α emission seen by Heckman et al. is used to estimate the resolved H α line flux, less than 5 per cent of the resolved K -band emission around 4C+09.17 could be due to this emission.

5 SUMMARY

Near-infrared images of the radio-loud quasar 4C+09.17 show the presence of three ‘companion’ objects with brightness of $17.9 < K < 20.2$ mag, as well as resolved, diffuse emission surrounding the quasar. The brightest of these components has been measured to have a redshift $z=0.8384$ (Lehnert & Becker 1997, in preparation) and is probably the galaxy responsible for the strong Mg II absorption seen in the spectrum of the quasar. The optical–infrared colours of this object are consistent with a late-type spiral galaxy at this redshift, with a luminosity of about $2L^*$. The second brightest companion at K appears most consistent with a star-forming galaxy at $z > 1.5$, and if it is at the redshift of 4C+09.17, it has an intrinsic luminosity of about $7L^*$. If, on the other hand, it is a spiral galaxy at $z \sim 1.5$, it may be associated with the weaker Mg II absorption-line system at $z=1.466$, and have a luminosity of about $2L^*$. The faintest member of the 4C+09.17 system have very blue $J-K$, yet red $V-J$ colours, which appear inconsistent with either an old or young stellar population at the absorption- or emission-line redshifts associated with 4C+09.17. The unusual colours and diffuse morphology of this component may be explained if it is a combination of strong line emission and scattered QSO light. The fact that it lies along the direction of the radio jet and the extended Ly α emission-line gas strengthens this interpretation. The diffuse emission surrounding 4C+09.17 is very bright ($K \sim 17.0$ mag) and redder than the QSO by about 1 mag in $J-K$. If this emission is starlight at the redshift of 4C+09.17, an elliptical host galaxy with a luminosity larger than about $40L^*$ is implied. Scattered and reddened AGN light, emission-line gas, and

flux from absorbing galaxies along the line of sight may all contribute to this emission.

ACKNOWLEDGMENTS

This work was based on observations made with the W. M. Keck Observatory, which is operated as a scientific partnership between the California Institute of Technology and the University of California. We thank the entire Keck staff, especially Wendy Harrison and Al Conrad, for making these observations possible. We also thank Peter Barthel, Tim Heckman, David Hogg, Neill Reid, Tom Soifer and Chuck Steidel for helpful discussions. Finally, we thank Steve Warren, the referee, whose comments and suggestions helped to improve the final version of this paper. Infrared astrophysics at Caltech is supported by grants from NASA. This research has made use of the NASA/IPAC Extragalactic Database, which is operated by the Jet Propulsion Laboratory, Caltech, under contract with NASA.

REFERENCES

- Aaronson M. A., 1977, PhD thesis, Harvard Univ.
- Bahcall J. N., Kirhakos S., Saxe D. H., Schneider D. P., 1997, *ApJ*, 479, 642
- Barthel P. D., Miley G. K., Schlizzi R. T., Lonsdale C. J., 1988, *A&AS*, 73, 515
- Barthel P. D., Tytler D. R., Thomson B., 1990, *A&AS*, 82, 339
- Boroson T. A., Oke J. B., 1984, *ApJ*, 281, 535
- Boroson T. A., Persson S. E., Oke J. B., 1985, *ApJ*, 293, 120
- Bruzual G. A., Charlot S., 1993, *ApJ*, 405, 538
- Burstein D., Heiles C., 1982, *AJ*, 87, 1165
- Carlberg R., Couchman H., 1989, *ApJ*, 340, 47
- Casali M. M., Hawarden T. G., 1992, *UKIRT Newsletter*, 3, 33
- Coleman G. D., Wu C.-C., Weedman D. W., 1980, *ApJS*, 43, 393
- de Vaucouleurs G., 1948, *Ann. D’Astrophys.*, 11, 247
- Disney M. J. et al., 1995, *Nat*, 376, 150
- Eales S. A., Rawlings S., 1993, *ApJ*, 411, 67
- Hartwick F., Schade D., 1990, *ARA&A*, 28, 437
- Heckman T. M., Lehnert M. D., van Breugel W., Miley G. K., 1991, *ApJ*, 370, 78
- Hutchings J. B., Morris S. C., 1995, *AJ*, 109, 1541
- Hutchings J. B., Crampton D., Campbell B., 1984, *ApJ*, 280, 41
- Kellerman K. I., Sramek R. A., Schmidt M., Schaffer D. B., Green R. F., 1989, *AJ*, 98, 1195
- Kormendy J., 1977, *ApJ*, 218, 333
- Lanzetta K., Bowen D., 1990, *ApJ*, 357, 321
- Lernert M. D., Heckman T. M., Chambers K. C., Miley G. K., 1992, *ApJ*, 393, 68
- Lonsdale C. J., Barthel P. D., Miley G. K., 1993, *ApJS*, 87, 63
- Malkan M. A., 1984, *ApJ*, 287, 555
- McCarthy P. J., 1993, *ARA&A*, 31, 639
- McCarthy P. J., Elston R., Eisenhardt P., 1992, *ApJ*, 387, L29
- McLeod K. K., Rieke G. H., 1995, *ApJ*, 454, L77
- Mobasher B., Sharples R. M., Ellis R. S., 1993, *MNRAS*, 263, 560
- Neugebauer G., Matthews K., Armus L., 1995, *ApJ*, 455, L123
- Rieke G. M., Lebofsky M. J., 1985, *ApJ*, 288, 618
- Savage B. D., Mathis J. D., 1979, *ARA&A*, 17, 73
- Schechter P., 1986, *ApJ*, 203, 297
- Schmidt M., Schneider D. P., Gunn J. E., 1995, *AJ*, 110, 68
- Schneider D. P., van Gorkom J. H., Schmidt M., Gunn J. E., 1992, *AJ*, 103, 1451
- Smith E. P., Heckman T. M., Bothun G., Romanishin W., Balick B., 1986, *ApJ*, 306, 64